Fluorine-induced *J*-aggregation enhances emissive properties of a new NLO push-pull chromophore

Chiara Botta,*[a] Elena Cariati,*[b] Gabriella Cavallo,[c] Valentina Dichiarante,[c] Alessandra Forni,*[d] Pierangelo Metrangolo,*[c] Tullio Pilati,[c] Giuseppe Resnati,*[c] Stefania Righetto,[b] Giancarlo Terraneo[c] and Elisa Tordin[b]

[a] ISMAC-CNR, via Bassini 15, 20133 Milan, Italy;

[b] Dept. Chemistry and INSTM UdR Milano, University of Milan, via Golgi 19, I-20133 Milan, Italy;

[c] NFMLab, DCMIC "Giulio Natta", Politecnico di Milano, via Mancinelli 7, I-20131 Milan, Italy;

[d] ISTM-CNR, University of Milan, via Golgi 19, I-20133 Milan, Italy;

*:

- Chiara Botta, ISMAC-CNR, via Bassini 15, 20133 Milan, Italy. Phone: +39 02 2369 9734, Fax: +39 02 7063 6400, e-mail: chiara.botta@ismac.cnr.it

- Elena Cariati, Dept. Chemistry and INSTM UdR Milano, University of Milan, via Golgi 19, I-20133 Milan, Italy. Phone: +39 02 50314370, Fax: +39 02 50314405, e-mail: elena.cariati@unimi.it

- Alessandra Forni, ISTM-CNR, University of Milan, via Golgi 19, I-20133 Milan, Italy. Phone: +39 02 50314273, Fax: +39 02 50314300, e-mail: alessandra.forni@istm.cnr.it

- Pierangelo Metrangolo, Giuseppe Resnati, NFMLab, Department of Chemistry, Materials, and Chemical Engineering ''Giulio Natta'', Politecnico di Milano, via Mancinelli 7, 20131 Milan, Italy. Phone: +39 02 23993041 (P. M.), +39 02 23993032 (G. R.), Fax: +39 02 23993180, E-mail: pierangelo.metrangolo@polimi.it (P.M.); giuseppe.resnati@polimi.it (G. R.).

Electronic Supplementary Information

Experimental procedures

Materials and methods

Commercial HPLC-grade solvents were used without further purification. Starting materials were purchased from Sigma Aldrich, Acros Organics and Apollo Scientific. Reactions were carried out in oven-dried glassware under a nitrogen atmosphere.

^{1}H NMR and ^{19}F NMR spectra were recorded at room temperature with a Bruker AV500 spectrometer. Unless otherwise stated, $CDCl_3$ was used as both solvent and internal standard in ^{1}H NMR spectra. For ^{19}F NMR spectra, $CDCl_3$ was used as solvent and $CFCl_3$ as internal standard. Spectra were acquired on sample with concentration ranging between 10^{-5} M to 5 x 10^{-3} M in order to study the intermolecular interactions occurring at different concentrations. No shift was detected in ^{19}F signals, proving the absence of significant intermolecular interactions.

Mass spectra were performed on a Finnigan MAT TSQ70 apparatus for EI, on a Agilent 6890 series GC / Agilent 5973 mass selective detector network for GC-MS, and on Bruker Esquire 3000 Plus spectrometer for ESI.

Dynamic light scattering (DLS) measurements were performed at 25°C on a Malvern Nanozetasizer instrument with a 633 nm He-Ne laser, on chloroform solutions with concentration ranging from 10^{-5} M to 5 x 10^{-3} M.

Attenuated total reflectance FTIR (ATR-FTIR) spectra were recorded on a Nicolet Nexus FTIR spectrometer equipped with a UATR unit. The values were given in wavenumbers and were rounded to 1 cm^{-1} upon automatic assignment.

Melting points were assigned through an Olympus BX51 polarized-light optical microscope equipped with a Linkam Scientific LTS 350 heating/cooling stage and a Sony CCD-IRIS/RGB color video camera connected to a Sony video monitor CMA-D2 (heating rate 10 °C/min).

Deoxycholic acid (DCA) was purchased from Sigma Aldrich and used without further purification. Films of DCA inclusion compound **1b-DCA** were obtained by casting **1b**/DCA mixtures with a 1:4 molar ratio, from THF solutions, following the procedure described in ref. S1.

Optical absorption measurements were performed with a Perkin-Elmer Lambda-9 spectrometer. Photoluminescence and photoluminescence excitation profiles were obtained with a SPEX 270 M

monochromator equipped with a N_2 cooled charge-coupled device, exciting with a monochromatic Xe lamp. All spectra were corrected for the instrument response. Solid state PL QY measurements were carried out using a home-made integrating sphere, according to a previously reported procedure.[S1]

EFISH NLO measurements were carried out in $CHCl_3$ and DMF solutions at different concentrations, at a nonresonant fundamental wavelength of 1907 nm, using a Q-switched, mode-locked Nd^{3+}:YAG laser. The 1064 nm initial wavelength was shifted to 1907 nm by a Raman shifter with a high-pressure H_2 cell.

Single crystal X-ray diffraction data were collected on a Bruker KAPPA APEX II diffractometer with Mo-Kα radiation and CCD detector. The structures were solved by SIR2002[S2] and refined by SHELXL-97[S3] programs, respectively. The refinement was carried on by full-matrix least-squares on F^2. Hydrogen atoms were placed using standard geometric models and with their thermal parameters riding on those of their parent atoms.

X-Ray Powder Diffraction (XRPD) measurements were performed with a Bruker AXS D8 powder diffractometer, using the following experimental parameters: Cu-Kα radiation (λ = 1.54056 Å); scanning interval: 5 - 40° 2θ; step size: 0.016°; exposure time: 1.5 s per step. The crystallite average sizes were then estimated for both samples through the Scherrer equation integrating the area underneath the XRD peak at 2θ = 12,84°. The peak position and the full-width at half maximum height (FWHM) of the peak were obtained using TOPAS software.

The milling was carried out in a high speed ball-milling apparatus for 10 min at 30 Hz.

Synthesis of 1b

Compound **1b** was synthesized following a previously reported procedure,[S4] as sketched in Scheme S1, and purified by silica gel chromatography, eluting with dichloromethane/hexane 2:3 mixture. Physical and spectroscopic data were in accordance with literature.[S4]

1b: m.p.= 209-215 °C; ^{1}H NMR ($CDCl_3$, 500 MHz): δ 7.53-7.47 (m, 5H), 7.43 (d, 2H, J = 5 Hz), 7.12-7.05 (m, 2H, d), 6.94-6.89 (m, 2H, d), 6.75 (m, 2H, d), 3.00 (s, 6H, CH_3). ^{19}F NMR ($CDCl_3$, 500 MHz): δ -144.4 (2F, m), -141.2 (2F, m). FT-IR (cm^{-1}): 2920, 2851, 1609, 1589, 1492, 1358, 1165, 1040, 961, 927, 813, 691.

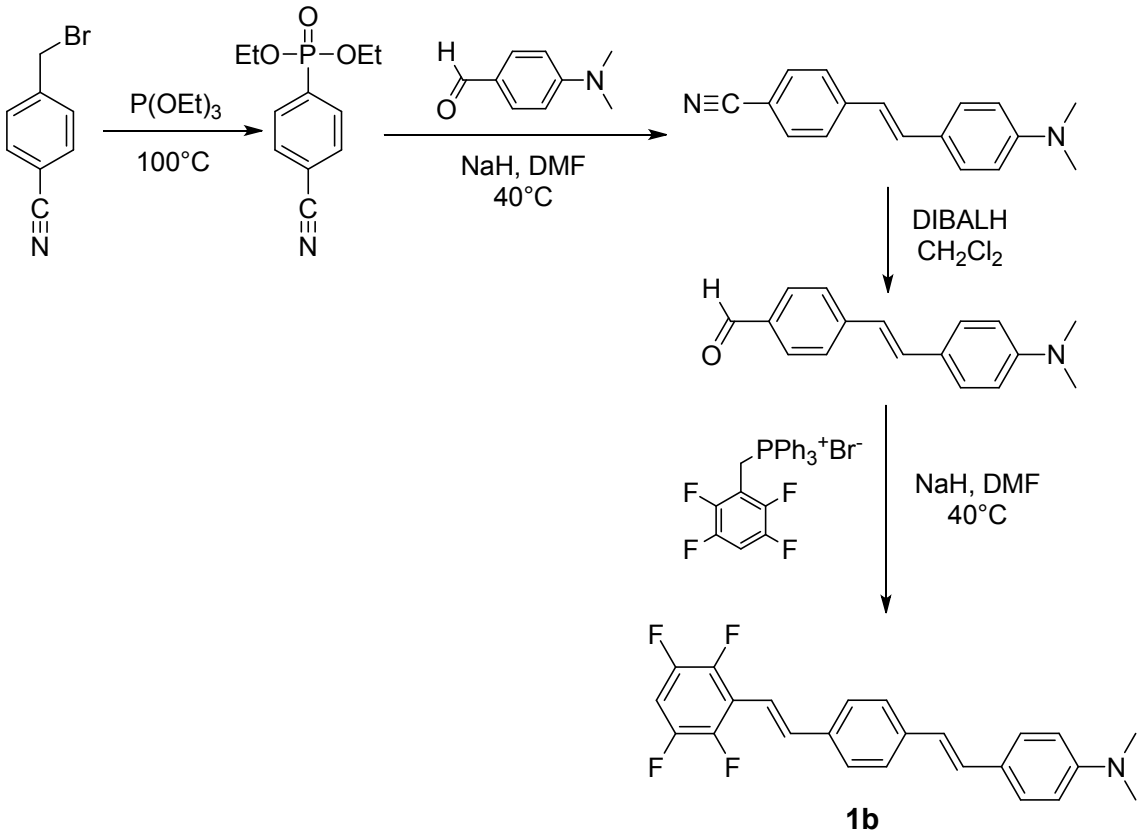

Scheme S1 Synthetic route to compound **1b**.

Optical measurements

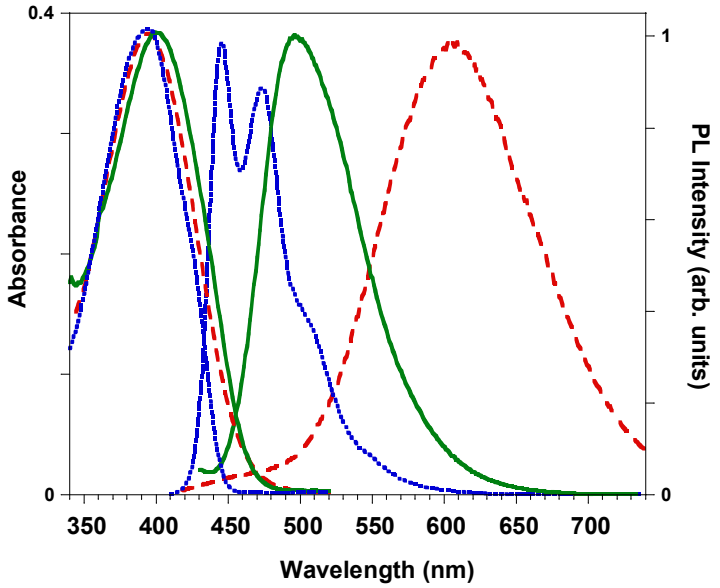

Fig. S1 Absorption and emission spectra of **1b** solutions, in pentane (blue dotted line), toluene (green solid line), and acetonitrile (red dashed line).

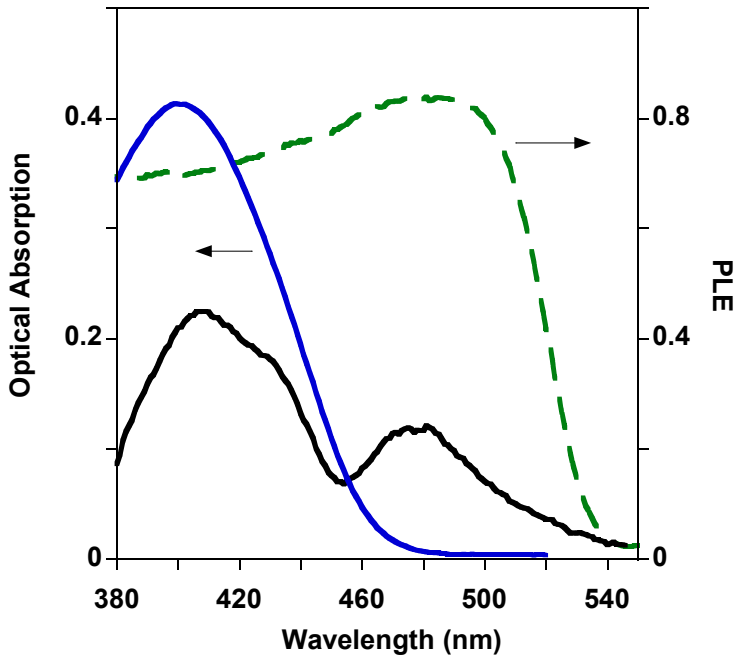

Fig. S2 Absorption spectra of: **1b** crystallized powder dispersed in nujol (black solid line), and dissolved in toluene (blue line); PL excitation spectrum (PLE) of the same powder (green dashed line).

Single crystal X-ray diffraction analysis

To collect data, we selected a crystal not too curved, and put it on a thin, rigid lamina obtained exploding on a cold marble slab a fused glass bubble. The crystal was mounted with a film of a highly dense perfluoropolyether, to prevent crystal gathering and data collection was carried on at low temperature (103 K), for several hours. The quality of our crystallographic data set was quite poor, but still enough to solve the structure. All heavy atoms were obtained by direct methods and difference map. Due to the low number of data and their low resolution, only fluorine atoms and the dimethylamino group were refined with anisotropic displacement parameters.

CIF containing crystallographic data can be obtained free of charge from the Cambridge Crystallographic Data Centre via www.ccdc.cam.ac.uk/data_request/cif (CCDC No. 961738).

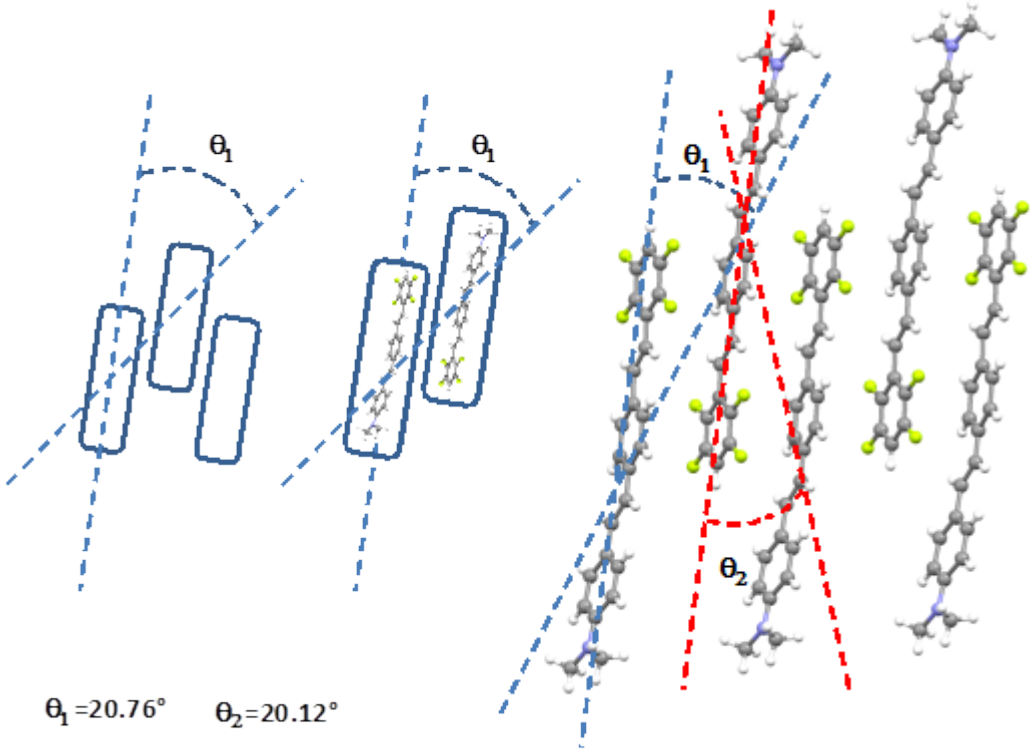

Fig. S3.: Slipped staking arrangement typical for J-aggregation and slip angles measured for **1b.**

Table S1. Crystallographic data for **1b** crystals.

Chemical Formula	$C_{24}H_{19}F_4N$
M_r	397.40
Crystal system, space group	Monoclinic, $P2_1/c$
Temperature (K)	103
a, b, c (Å)	7.594 (5), 5.874 (4), 41.51 (3)
β (°)	94.302 (8)
V (Å^3)	1846 (2)
Z	4
Radiation type	Mo $K\alpha$
μ (mm^{-1})	0.11
Crystal size	0.28 × 0.14 × 0.01
Data collection	
Diffractometer	Bruker *APEX*-II CCD area detector diffractometer
Absorption correction	-
No. of measured, independent and observed [$I > 2\sigma(I)$] reflections	5727, 1814, 1100
R_{int}	0.083
θ_{max} (°)[a]	20.8
Refinament	
$R[F^2 > 2\sigma(F^2)]$, $wR(F^2)$, S	0.113, 0.294, 1.07
No. of reflections	1814
No. of parameters	155
No. of restraints	0
No. of H-atom treatment	H-atom parameters constrained
	$w = 1/[\sigma^2(F_o^2) + (0.1036P)^2 + 19.5133P]$ where $P = (F_o^2 + 2F_c^2)/3$
$\Delta\rho_{max}$, $\Delta\rho_{min}$ (e Å^{-3})	0.50, −0.37

[a] The crystals were always twinned and/or curved. The sample chosen was apparently the best for dimensions and diffraction quality. It was put on a very thin, rigid lamina obtained exploding a bubble of fused glass; the crystal was fixed on the lamina through a film of a highly dense perfluorinated compound; this technique assured a good adhesion between glass and crystal and prevented the crystal curvature increasing during the freezing process. In spite of the long time of data collection (120"/frame), it was impossible to collect data at θ > 21°. Moreover, due to the very anisotropic form of the spot, probably caused by the curvature of the crystal, a number of reflections were not integrated, so that the data quality was very poor and the resolution was low. Nethertheless, the structure solution was easy, leaving no doubt about its correctness.

X-Ray Powder Diffraction (XRPD) analysis

a)

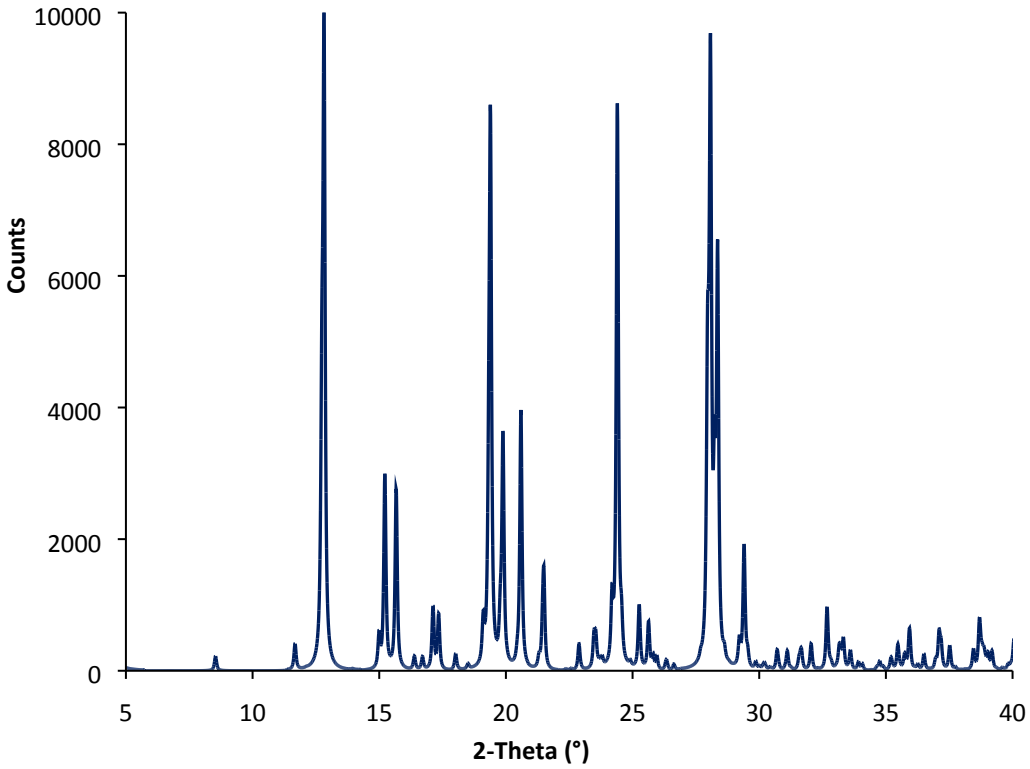
10000
8000
6000
4000
2000
0
Counts
5
10
15
20
25
30
35
40
2-Theta (°)

b)

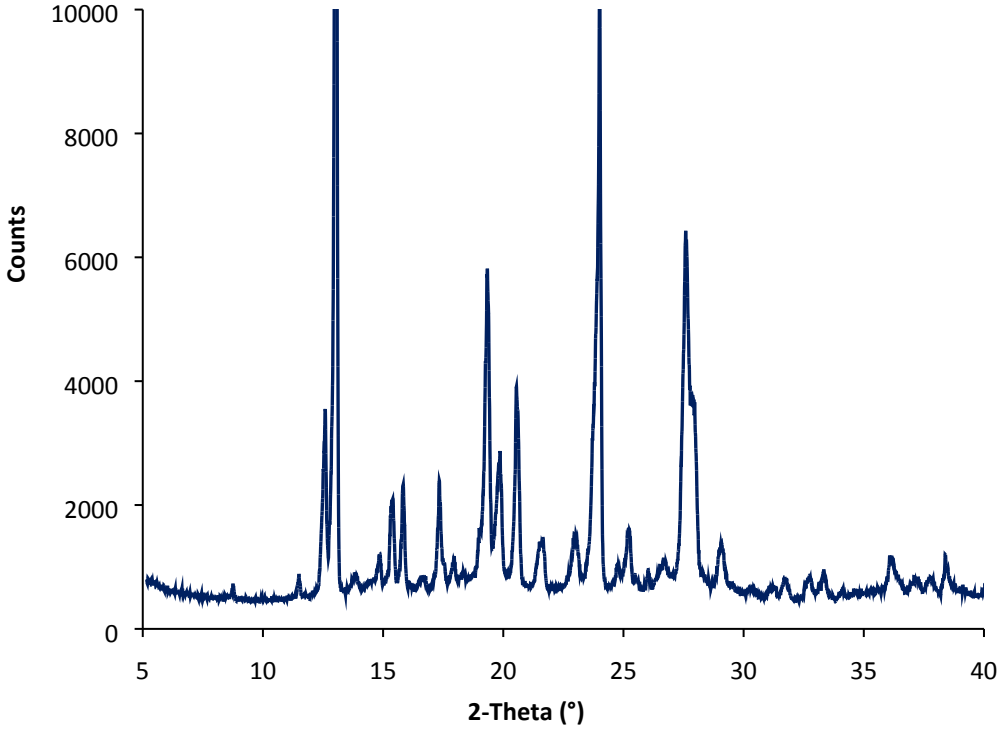
10000
8000
6000
4000
2000
0
Counts
5
10
15
20
25
30
35
40
2-Theta (°)

c)

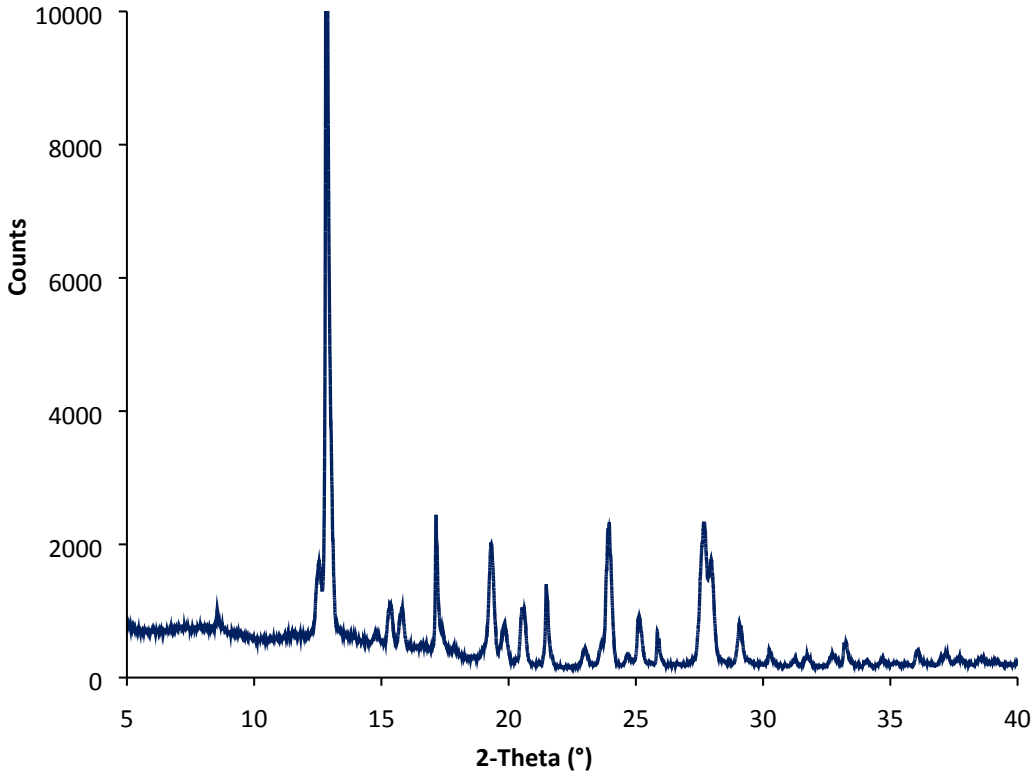

Fig. S4 PXRD patterns of: (a) **1b**, simulated from single crystal X-ray structure; (b) **1b**, native powder; (c) **1b**, powder obtained by fast precipitation from chloroform solution.

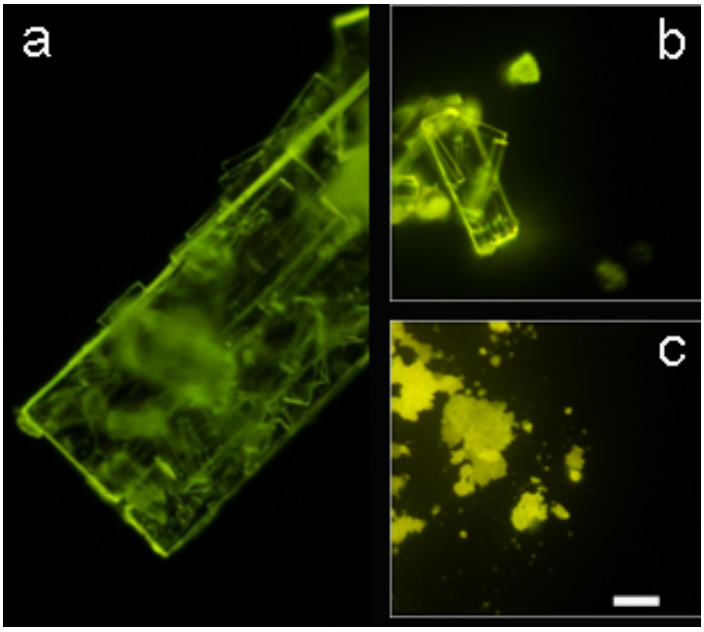

Fig. S5 Fluorescence Microscopy images of **1b** native powder (a); **1b** powder obtained by fast precipitation before (b) and after (c) grinding. Scale bar is 20 μm long for all the panels

Computational details

All calculations were performed with the Gaussian suite of programs.[S5]

The molecular structure of compound **1b** has been optimized *in vacuo* within the DFT approach, using the 6-311++G(d,p) basis set and the PBE0 functional,[S6,S7] which was previously judged well suited for describing the electronic and optical features of a series of organic dyes.[S8] The X-ray diffraction structure was used as starting point for geometry optimization. Using the PBE0/6-311++G(d,p) optimized geometry, standard vertical TD-PBE0/6-311++G(d,p) calculations[S9-S11] were carried out to determine the absorption wavelengths. In Table S1 we report the values of computed electronic and optical properties of **1b** compared with those of **1a**, as determined at the same level of theory.

Geometry optimization of dimers of compound **1b** in different arrangements were carried out *in vacuo* with the 6-31++G(d,p) basis set, using the B97D functional.[S12] Such functional has been chosen owing to the dispersive nature of the π-π interactions implied in these dimers, as denoted by the short C···C intermolecular distances observed in crystal structure (shortest intermolecular contacts: C2···C12$_{-x,1-y,2-z}$, 3.326 Å, and C9···C5$_{1-x,1-y,2-z}$, 3.379 Å). Preliminary test calculations on the dimers were also performed with the same functional used for the monomer, PBE0, but in all cases convergence problems were encountered. The computed interaction energies were corrected for basis set superposition error by the counterpoise technique.[S13]

Figure S5 shows the optimized dimer in the antiparallel J arrangement, mimicking that 'extracted' from the crystal structure. In such optimized dimer, the molecules, while shifted according to the J arrangement, are essentially overlapped along their long axis allowing to optimize both aryl-fluoroaryl quadrupolar electrostatic interactions and dispersive contributions. On the other hand, in the crystal structure, adjacent molecules within a π-π overlapped pile show as well a lateral shift as a consequence of stabilizing side-to-side interactions, which are not taken into account in DFT calculations. Such lateral shift explains the quite large values observed for the distances between centroids of fluorinated and hydrogenated rings, equal to 3.772 and 3.829 Å, if compared with the shortest C···C intermolecular contacts (see above). As a result, such centroids distances are reproduced by calculations with accuracy somewhat lower than that related to the shortest C···C contacts (about 0.26 against 0.15 Å, respectively. See Figure S5 for the relevant intermolecular distances within the computed dimer).

Table S1. Computed ground state dipole moments (μ, D) and electronic transitions (λ_{max}, nm), along with the associated excited state dipole moments (μ_e, D), the transition dipole moments (μ_{eg}, D) and the oscillator strengths (f), for compounds **1a** and **1b**[a]

Compound	μ	λ_{max}	μ_e	μ_{eg}	f
1a	7.62	460	26.61	12.70	1.65
1b	6.54	449	24.23	12.03	1.52

[a]Ground state properties and electronic transitions computed *in vacuo* at respectively PBE0/6-311++G(d,p) and TD PBE0/6-311++G(d,p) level with Gaussian09, rev. C.01.

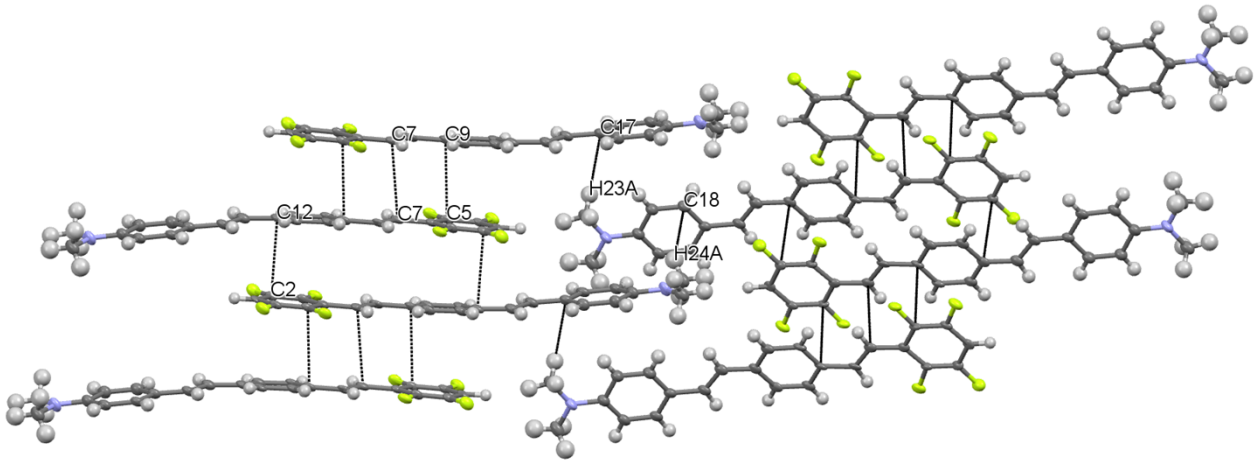

Fig. S6. A cluster of **1b** molecules , showing the shortest π-π and methyl···π interactions as dotted lines

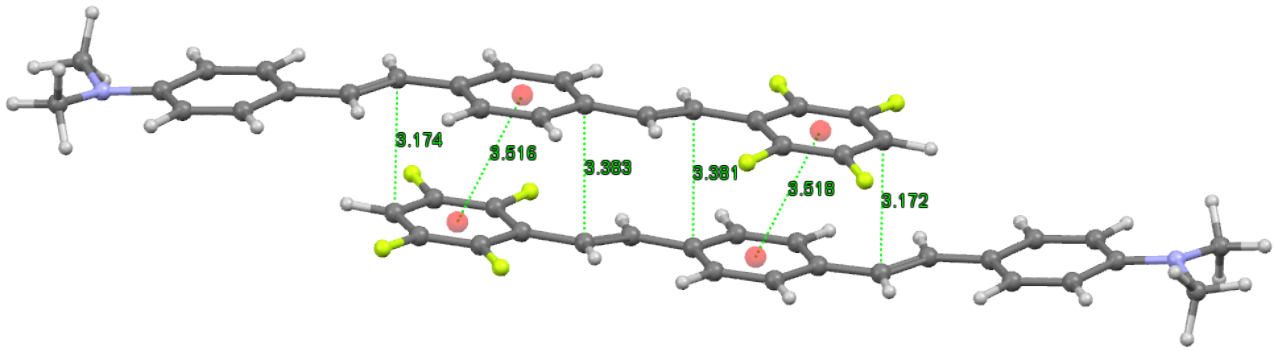

Fig. S7. Plot of the optimized B97D/6-31++G(d,p) dimer of compound **1b** in the J antiparallel arrangement, showing selected intermolecular C···C contacts and the distances between the centroids of the fluorinated rings and those of the hydrogenated ones.

References

S1 J. Moreau, U. Giovanella, J.-P. Bombenger, W. Porzio, V. Vohra, L. Spadacini, G. Di Silvestro, L. Barba, G. Arrighetti, S. Destri, M. Pasini, M. Saba, F. Quochi, A. Mura, G. Bongiovanni, M. Fiorini, M. Uslenghi and C. Botta, *ChemPhysChem*, 2009, **10**, 647.

S2 M. C. Burla, M. Camalli, B. Carrozzini, G. L. Cascarano, C. Giacovazzo, G. Polidori and R. Spagna, *J. Appl. Cryst.*, 2003, **36**, 1103.

S3 G. M. Sheldrick, *Acta Cryst.*, 2008, **A64**, 112.

S4 E. Cariati, G. Cavallo, A. Forni, G. Leem, P. Metrangolo, F. Meyer, T. Pilati, G. Resnati, S. Righetto, G. Terraneo and E. Tordin, *Cryst. Growth Des.*, 2011, **11**, 5642.

S5 *Gaussian 09, Revision C.01*, M. J. Frisch *et al.*, Gaussian, Inc., Wallingford CT, 2011.

S6 M. Ernzerhof and G. E. Scuseria, *J. Chem. Phys.*, 1999, **110**, 5029.

S7 C. Adamo and V. Barone, *J. Chem. Phys.*, 1999, **110**, 6158.

S8 D. Jacquemin, E. A. Perpète, G. E. Scuseria, I. Ciofini and C. Adamo, *J. Chem. Theory Comput.*, 2008, **4**, 123; D. Jacquemin, V. Wathelet, E. A. Perpète and C. Adamo, *J. Chem. Theory Comput.*, 2009, **5**, 2420.

S9 E. Runge, E. K. U. Gross, *Phys. Rev. Lett.* 1984, **52**, 997.

S10 R. E. Stratmann, G. E. Scuseria and M. J. Frisch, *J. Chem. Phys.*, 1998, **109**, 8218.

S11 M. E. Casida, *J. Mol. Struct. (THEOCHEM)*, 2009, **914**, 3.

S12 S. Grimme, *J. Comput. Chem.*, 2006, **27**, 1787.

S13 S. F. Boys and F. Bernardi, *Mol. Phys.*, 1970, **19**, 553.